8A.4. THE SENSITIVITY OF SIMULATED CONVECTIVE STORMS TO VARIATIONS IN PRESCRIBED MICROPHYSICS PARAMETERS

Charles Cohen* and Eugene W. McCaul, Jr.
Universities Space Research Association
Huntsville, Alabama

1. INTRODUCTION

Any parameterization of microphysical processes requires that some physical quantities be specified. In the RAMS model (Pielke *et al.* 1992; Walko *et al.* 1995), hydrometeors in each category are described by a gamma distribution

$$n(D) = \frac{N_t}{\Gamma(\nu)} \left(\frac{D}{D_n}\right)^{\nu-1} \frac{1}{D_n} exp\left(-\frac{D}{D_n}\right) \qquad (1)$$

where the number density n is a function of diameter, D. Here, N_t is the number concentration, Γ is the gamma function, ν is the shape parameter of the gamma distribution, and D_n is the characteristic diameter. Using the equation

$$\overline{m} = \frac{\rho_a r}{N_t} \qquad (2)$$

where $\overline{m}$ is mean mass of the hydrometeor category, ρ_a is the air density, and r is the mixing ratio, it becomes apparent that only two of the three quantities, ν, N_t and D_n, must be specified in a simulation that does not forecast N_t. A standard practice in RAMS has been to specify, instead of D_n, the diameter of the particle with mean mass, $D_{\overline{m}}$. This can be related to D_n by using Eq. 5 of Walko et al. (1995) to express the mean mass of the hydrometeor category as

$$\overline{m} = \alpha_m {D_n}^{\beta_m} \frac{\Gamma(\nu+\beta_m)}{\Gamma(\nu)} = \alpha_m {D_{\overline{m}}}^{\beta_m} \qquad (3)$$

where the mass of a particle with diameter D is $\alpha_m D^{\beta_m}$. We are continuing the work of McCaul and Cohen (2002), who used $\nu = 1.5$, and the default values of $D_{\overline{m}}$ in RAMS of 0.1 cm for rain and graupel and 0.3 cm for hail. Hail is conventionally defined as having a diameter of at least 0.5 cm (Glickman 2000). However, as Meyers *et al.* (1997) explain, the mean diameter of hail in RAMS is smaller than would be expected because the hail category in the model also takes into account frozen drops, which are smaller than hail. Truncating the hail size distribution at 0.5 cm, as suggested by Curic and Janc (1997), would therefore not be appropriate in RAMS.

2. METHODOLOGY

*Corresponding author address: Charles Cohen, Universities Space Research Association, 6700 Odyssey Drive, Suite 203, Huntsville, AL 35806, E-mail: cohen@space.hsv.usra.edu

In this study, we use version 3b of the RAMS model, configured as in McCaul and Cohen (2002), but with a number of modifications and improvements, which are listed in McCaul *et al.* (2004). In addition to solving for the three Cartesian velocities, ice-liquid water potential temperature (Tripoli and Cotton 1981), and pressure, the model also forecasts mixing ratios of rain, hail, graupel, pristine ice, snow, and aggregates, and employs a diagnostic equation to obtain temperature and the mixing ratios of water vapor and cloud water. Particle number concentration is forecast for pristine ice.

We use RAMS with a square domain, 75 km on a side, with a horizontal grid interval of 500 m, and a vertically stretched grid with spacing ranging from 250 m at the ground to 750 m at 20 km in altitude. The sounding (Fig. 1) used in the horizontally uniform initial state has a convective available potential energy (CAPE) of 2000 J kg^{-1}, an LCL of 1.6 km, and a semicircular hodograph with a radius of 12 m s^{-1}. Convection is initiated with a spheroidal warm bubble, as in McCaul and Cohen (2002).

We experiment with the model by changing ν in (1) for precipitating hydrometeor species from the 1.5 used in our previous work to 5, and separately by increasing $D_{\overline{m}}$ by 150% to 0.25 cm for graupel and 0.75 cm for hail, leaving $D_{\overline{m}}$ unchanged for other species. RAMS computes the rate of collection of hydrometeors with a look-up table. The tables are correct for $\nu = 1.5$, but for the present study we recomputed the collection tables for all other values of ν, so that they more closely conform to the stochastic collection equation (Eq. 46 of Walko *et al.* 1995).

3. RESULTS AND DISCUSSION

Multiplying $D_{\overline{m}}$ by 2.5 for hail and graupel makes more of a difference in the simulations than does increasing ν from 1.5 to 5 for rain, hail, graupel, snow, and aggregates. We begin by explaining why the results are not very sensitive to the value of ν, and then we compare simulations with different values of $D_{\overline{m}}$.

Fig. 2a shows four gamma distributions of hailstones, all with a mass density of 1 g m^{-3}, for the shape parameter, ν, equal to 1.5 and 5, and for $D_{\overline{m}} = 0.30$ cm (the default value) and 0.75 cm. Increasing ν produces a narrower and less positively skewed distribution with fewer small particles and fewer large particles.

Next, we compute the rate of collection of cloud water by a hailstone of each diameter, using a cloud droplet number concentration of 300 cm^{-3} (the default

value in RAMS), and radius of 10 μm. (In this calculation, we use 1.0 for the collection efficiency, because it is not a function of the diameter of the hail in RAMS.) When this is multiplied by the size distributions, we obtain collection densities (Fig. 2b), showing the rate of collection of cloud droplets as a function of the diameter of the hailstone. The areas under these curves are the total collection rates. Hailstones smaller than 0.1 cm collect very little cloud water, even when, with $\nu = 1.5$, they are present in large numbers. Increasing ν from 1.5 to 5 causes only a 14% increase in the collection rate, because with $\nu = 1.5$ the small number of hailstones larger than 0.6 cm have large rates of collection.

Averaged over space and time during the second hour of the simulations, the most prominent effect of increasing ν from 1.5 to 5 is a greater evaporation of rain (not shown), leading to a larger ratio of downdraft mass flux to updraft mass flux in the lower troposphere (Fig. 3a) and less precipitation at the ground. The differences in the precipitation rates are not large because, as we have seen, there is a larger collection rate with the larger ν. Fig. 3b depicts the microphysical precipitation efficiency by comparing the sum of autoconversion and collection of cloud water to the homogeneous freezing of cloud water. We see that the magnitude of the homogeneous freezing of cloud water is almost unchanged when ν is increased, despite the greater updraft mass flux and greater conversion of cloud water to precipitation with a larger ν.

Increasing $D_{\overline{m}}$ by 150% decreases the collection rate (the area under the curves in Fig. 1b) by 37%, for either value of ν. Qualitatively, this should be expected; for a single hailstone of diameter D, the collection rate is very close to being proportional to $D^{2.5}$ (the terminal velocity, which is proportional to the square root of the diameter, multiplied by the cross-sectional area), while the mass is proportional to D^3. Larger hailstones, therefore, have lower collection rates per unit mass. This is largely compensated by the fact that, when less cloud water is collected by hail, there is more of it available to be collected by graupel, whose peak concentration is at a slightly higher altitude. Still, the microphysical precipitation efficiency is smaller with the larger $D_{\overline{m}}$ (Fig. 3b).

In contrast to the simulations of van den Heever and Cotton (2004), the speed and direction of storm propagation can be significantly affected by the size of the hydrometeors. Fig. 4 shows horizontal fields near the ground at 45 min, just as the propagation of the storms in the two simulations are beginning to differ. With the smaller hail and graupel, the precipitation is advected farther ahead of the gust front, evaporating in the undisturbed air. Although this does not change the equivalent potential temperature, it does cool the air ahead of the gust front, increasing its density and inhibiting its lifting to its LCL. Ten minutes later (not shown), it is only with the larger hail that an additional updraft has formed at the gust front between the left- and right-movers. This soon joins with the right-mover, effectively forming a storm with a downdraft beneath the updraft (Fig. 5), and centered slightly to its south, in contrast to the storm with the smaller hail, where the downdraft, which is northwest of the updraft, is driving the updraft toward the southeast relative to the moving domain. Relative to the ground, the average propagation of the right-movers during the second hour of the simulations is 4.66 m s^{-1} at -5.9° with the smaller hail and 9.15 m s^{-1} at -27° with the larger hail.

4. ACKNOWLEDGMENTS

This research is a part of the COnvection Morphology PArameter Space Study (COMPASS), which is supported by grant ATM-0126408 from the National Science Foundation under the supervision of Dr. Stephan Nelson. For additional information, see http://space.hsv.usra.edu/COMPASS.

5. REFERENCES

Curic, M., and J. Janc, 1997: On the sensitivity of hail accretion rates in numerical modeling. *Tellus*, **49A**, 100–107.

Glickman, T. S. Ed., 2000: Glossary of Meteorology. 2d ed. Amer. Meteor. Soc., 855 pp.

McCaul, E. W. Jr., and C. Cohen, 2002: The impact on simulated storm structure and intensity of variations in the mixed layer and moist layer depths. *Mon. Wea. Rev.*, **130**, 1722–1748.

——, ——, and C. Kirkpatrick, 2004: The sensitivity of simulated storm structure and intensity to the temperature at the lifted condensation level. submitted to *Mon. Wea. Rev.*

Meyers, M. P., R. L. Walko, J. Y. Harrington, and W. R. Cotton, 1997: New RAMS cloud microphysics parameterization. Part II: The two-moment scheme. *Atmos. Res.*, **45**, 3–39.

Pielke, R. A., W. R. Cotton, R. L. Walko, C. J. Tremback, W. A. Lyons, L. D. Grasso, M. E. Nicholls, M. D. Moran, D. A. Wesley, T. J. Lee, and J. H. Copeland, 1992: A comprehensive meteorological modeling system - RAMS. *Meteor. Atmos. Phys.*, **49**, 69–91.

Tripoli, G. J., and W. R. Cotton, 1981: The use of ice-liquid water potential temperature as a thermodynamic variable in deep atmospheric models. *Mon. Wea. Rev.*, **109**, 1094–1102.

Van den Heever, S., and W. R. Cotton, 2004: The impact of hail size on simulated supercell storms. *J. Atmos. Sci.*, **61**, 1596–1609.

Walko, R. L., W. R. Cotton, M. P. Meyers, and J. Y. Harrington, 1995: New RAMS cloud microphysics parameterization. Part I: the single-moment scheme. *Atmos. Res.*, **38**, 29–62.

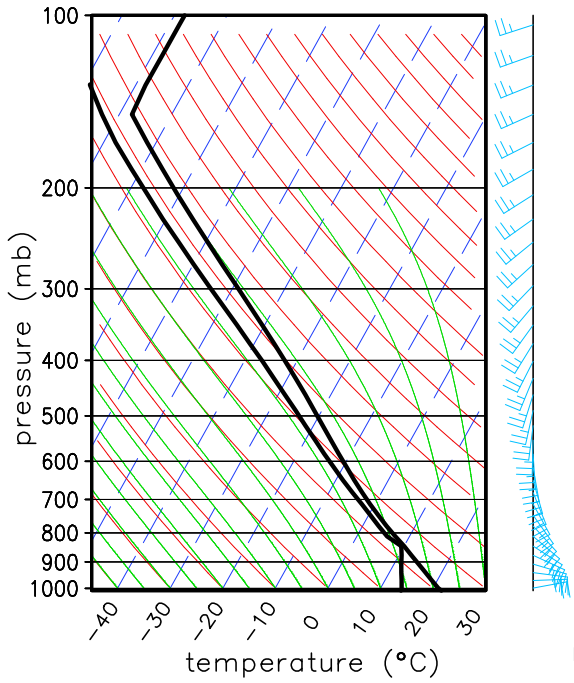

Fig. 1. Initial sounding

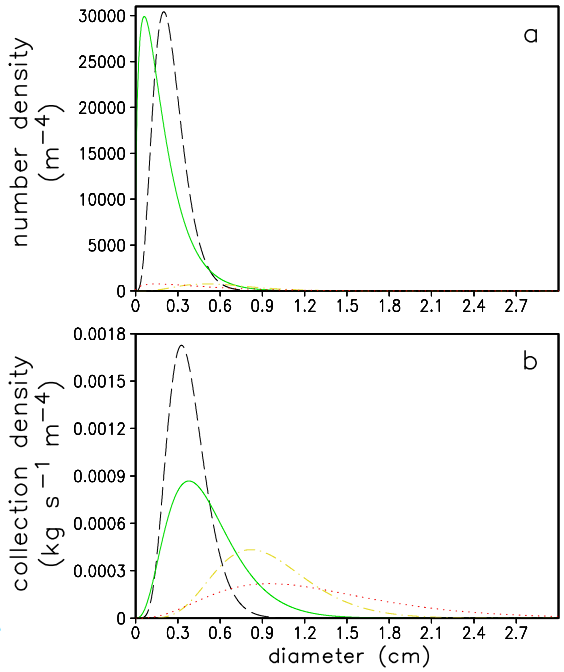

Fig. 2. Size distribution of hailstones (a) for $D_{\overline{m}}$ =0.30 cm, for ν=1.5 (solid) and ν=5 (dashed), and for $D_{\overline{m}}$ =0.75 cm, for ν=1.5 (dots) and ν=5 (dot−dash). Collection density of cloud droplets (b) for the distributions of hailstones shown above (kg s^{-1}m^{-4}, where the collection rate is in kg m^{-3}s^{-1}).

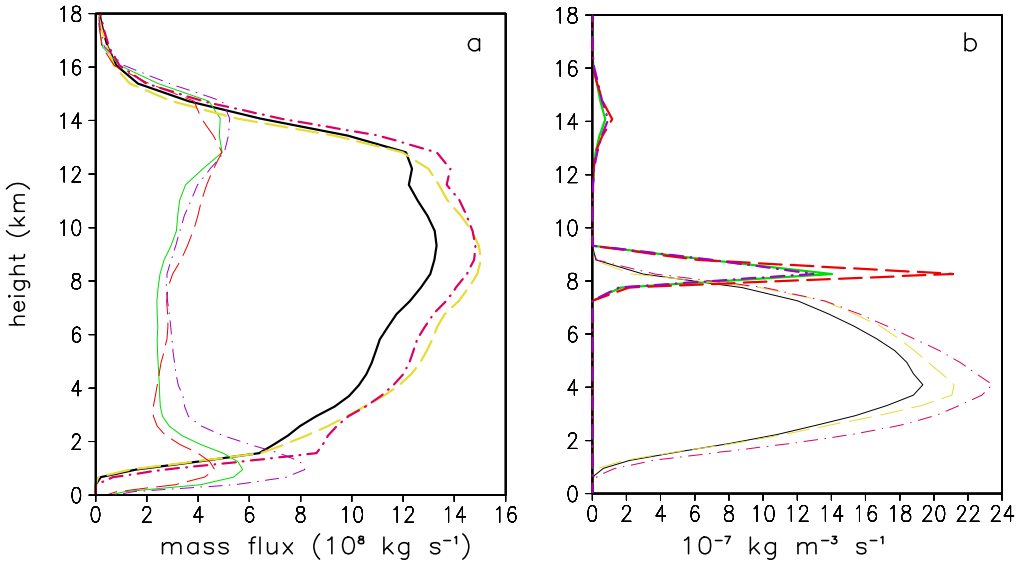

Fig. 3. Updraft (thick) and downdraft (thin) mass flux (a); autoconversion plus collection of cloud water (thin) and homogeneous freezing (thick) of cloud water (b); for the control (solid), $D_{\overline{m}}$ =0.75 cm (dashed), and ν=5 (dot−dash). All quantities are averaged over the whole domain during the second hour.

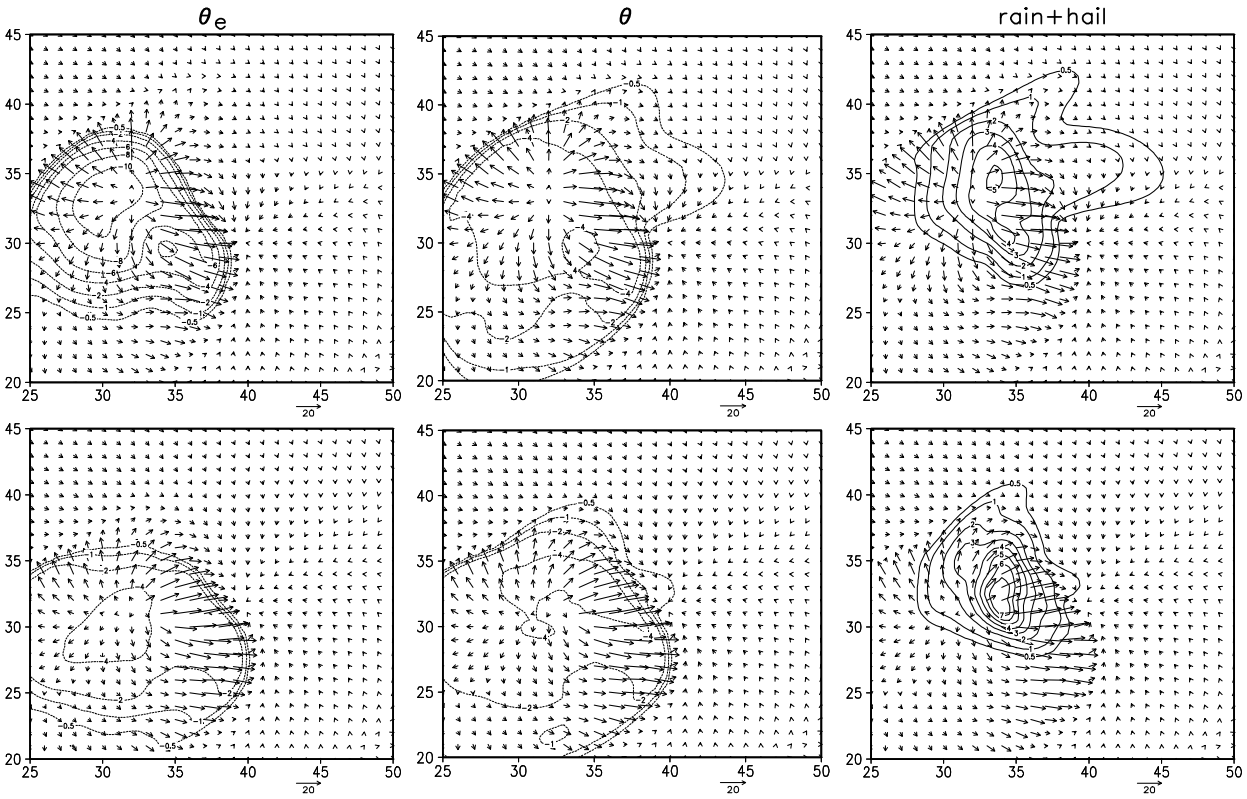

Fig. 4. Perturbation wind vectors at every other grid point with perturbation θ_e (left), perturbation θ (middle), and rain + hail mixing ratio (g kg^{-1}) (right), all at 127 m at 45 minutes, for $D_{\overline{m}}$ =0.30 cm (top) and $D_{\overline{m}}$ =0.75 cm (bottom). Axes are labelled in km. For θ_e and θ, the contour interval is 2 with additional contours at −1 and −0.5, with the zero and positive contours omitted; for rain + hail, the contour interval is 1, with an additional contour at 0.5, with the zero contour omitted.

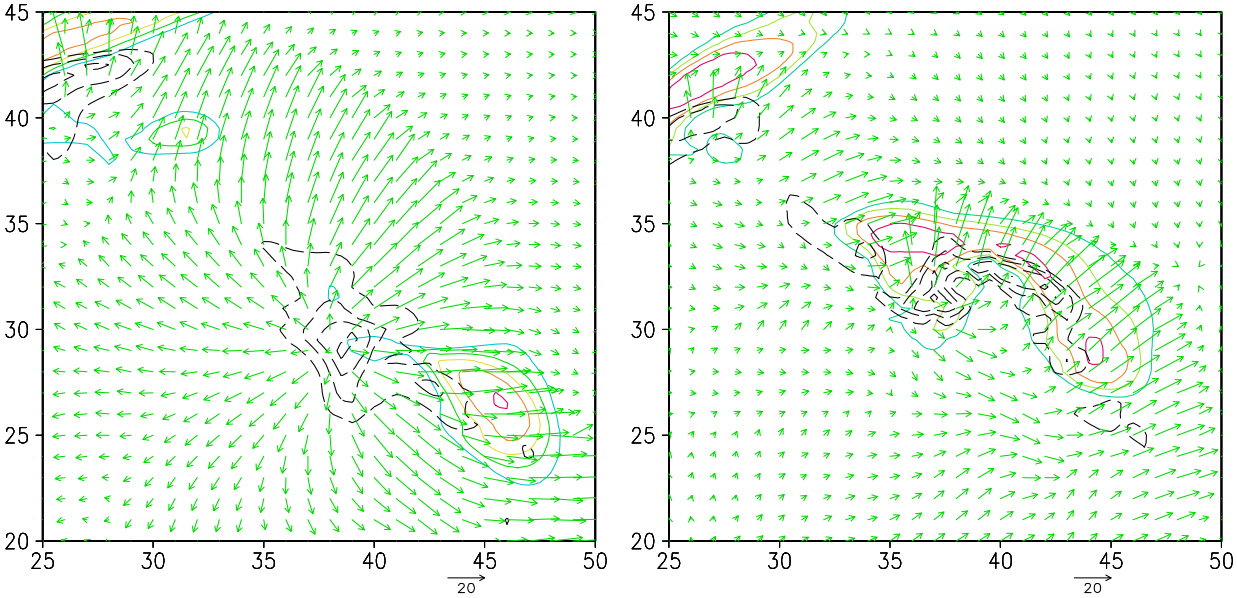

Fig. 5. Upward vertical velocity at 3.5 km (solid contours, interval 4 m s^{-1}, starting at 4 m s^{-1}); downward vertical velocity at 500 m (dashed contours, interval 2 m s^{-1}, with $w > -2$ m s^{-1} omitted); and perturbation wind vectors at every other grid point at 127 m; all at 75 minutes; for $D_{\overline{m}}$ =0.30 cm (left) and $D_{\overline{m}}$ =0.75 cm (right).